

# Preparation and characterisation of diopside-based glass–ceramic foams

S. Hasheminia<sup>a,\*</sup>, A. Nemati<sup>b</sup>, B. Eftekhari Yekta<sup>c</sup>, P. Alizadeh<sup>d</sup>

<sup>a</sup> Department of Materials Science and Engineering, Science and Research Branch, Islamic Azad University, Tehran, Iran

<sup>b</sup> Materials Science and Engineering Department, Sharif University of Technology, Azadi St., Tehran, Iran

<sup>c</sup> Ceramic Division, Department of Materials, Iran University of Science and Technology, Tehran, Iran

<sup>d</sup> School of Engineering, Tarbiat Modares University, Tehran, Iran

Received 13 July 2011; received in revised form 11 October 2011; accepted 12 October 2011

Available online 18 October 2011

## Abstract

Foaming and crystallisation behaviours of compacted glass powders based on a diopside glass–ceramic composition were investigated using the sintering route. The foaming agent was 2 wt.% SiC particles. The effect of PbO on the foaming ability of glasses was investigated. The results showed that the addition of PbO not only improved the foaming ability, by improving the wettability of the glass–SiC particles but also increased the crystallisation temperature and widened the temperature interval between the dilatometric softening point and the onset of crystallisation. The glass–SiC wetting angle was decreased from 85° for the lead-free glass, to 55° for the glass that contains 15 wt.% PbO.

© 2011 Elsevier Ltd and Techna Group S.r.l. All rights reserved.

**Keywords:** A. Sintering; Glass–ceramic foam; Diopside

## 1. Introduction

Glass foam has a unique combination of properties, such as lightweight, suitable rigidity, compression resistance, thermal insulation, freeze tolerance, nonflammability, chemical inertness and nontoxicity, rodent and insect resistance, bacteria resistance and water and steam resistance. Moreover, glass foam facilitates a quick construction and has low transport costs. It is easy to handle, cut, and drill and is readily combined with concrete. This combination of properties makes glass foam practically irreplaceable both in construction, e.g., for the insulation of roofs, walls, floors, and ceilings under hot or cold conditions, and in many other fields. Commercial glass foams exhibit porosity, apparent density and compressive strength values of approximately 85–95 vol%, 0.1–0.3 g/cm<sup>3</sup> and 0.4–6 MPa, respectively [1].

The cost of glass foam has been a key disadvantage for its use in the building industry. To reduce production costs, several modifications have been applied to both the processing techniques and the starting materials of glass foams.

The direct introduction of gases, i.e., blowing into molten glass, a technique dating back to the 1930s [2], was substituted by a sintering approach using a fine glass powder, which is converted to a pyro-plastic mass after being subjected to a proper heat treatment. The mass is then foamed by the development of gases, produced from the decomposition or oxidation of specific powder additives called “foaming agents” [3]. This processing allows significant energy saving because the viscous flow occurs at much lower temperatures than those required by the blowing [4].

Later, recycled glass [3–6] and industrial wastes, such as panel glass from dismantled cathode ray tubes [7–14], mining residues from feldspar excavation, oil shale [15], incinerator fly ash [16–18], coal ash [19,20] and metallurgical slag [21], were employed for manufacturing glass foam by the sintering route.

The preparation of a desirable foam glass requires a glass with a low tendency to crystallise [17,22,23] as well as a wide range of working temperatures [23]. Crystals affect the apparent viscosity of the glass and its foaming behaviour. Furthermore, crystals influence the structural integrity of the foam because of the mismatch of the thermal expansion coefficients. This can result in opening or cracking of the lamellae between adjacent bubbles, which reduces the insulation behaviour and enhances further coalescence of the bubbles during foaming. The coalescence phenomenon can reduce the strength of the foam glass

\* Corresponding author. Fax: +98 4114439058.

E-mail addresses: [s.hasheminia@yahoo.com](mailto:s.hasheminia@yahoo.com), [s.hasheminia@srbiau.ac.ir](mailto:s.hasheminia@srbiau.ac.ir) (S. Hasheminia).

considerably [17]. A number of recent papers [4,7,8,15,19–21] have examined the feasibility of preparing glass–ceramic foams. One can improve the mechanical properties of glass foam by reducing or eliminating the above mentioned problem.

Inexpensive and strong glass–ceramics can be produced by using the  $\text{SiO}_2\text{--Al}_2\text{O}_3\text{--CaO--MgO}$  glass system. Diopside, a crystalline phase that generally precipitates in these glasses, is responsible for the superior mechanical properties of the product. The diopside-based glass system has been used extensively to prepare of pore-free specimens [24–27]; however, based on our literature survey, there is no published work denoting that it has been used for the preparation of glass–ceramic foam.

In the present study, the effect of  $\text{PbO}$  on the foaming ability of a diopside-based glass was studied. Thus, the sintering and crystallisation behaviours of the  $\text{SiC}$ -bearing and  $\text{SiC}$ -free specimens as well as the chemical reactions that occur at the glass– $\text{SiC}$  interfaces were considered.

## 2. Experimental procedure

The base glass composition ( $F$ ) was chosen from a previous work [27], and the raw materials used were reagent-grade chemicals with a purity of >99 wt.%. The chemical composition of the investigated glasses is presented in Table 1.

The thoroughly mixed batches were melted into zircon crucibles in an electric furnace at 1450 °C for 2 h. The glass melts were then quenched in cold distilled water. The obtained glass frits were ground in an electric hard porcelain mortar for 2 h. The particle size measurements of the powdered glasses, which were carried out by a laser particle size analyser (Fritsch Analysete 22), showed a mean particle size of approximately 4.5  $\mu\text{m}$ .

A commercial-grade silicon carbide powder with a mean particle size of 12  $\mu\text{m}$  was used as a foaming agent, and 2 wt.%  $\text{SiC}$  was mixed with the above mentioned ground frits in an electric hard porcelain mortar for 15 min. The mixture was shaped into cylindrical pellets of 22 mm in diameter and 6 mm in thickness using a laboratory uniaxial press under a pressure of 40 MPa. The pellets were dried at 100 °C and then fired in an electric laboratory furnace in the temperature range of 850–1000 °C. A heating rate of 10 °C/min and a soaking time of 1 h were used for this step. The bulk and true densities of specimens were determined by considering their weights and dimensions and via the pycnometry method. The total porosity ( $P$ ) and foaming factor ( $\alpha$ ) of the fired specimens were calculated according to the following equations, respectively:

$$\%P = (1 - d_b/d_r) \times 100$$

Table 1  
Chemical composition of glasses (weight ratio).

Glass	$\text{SiO}_2$	$\text{Al}_2\text{O}_3$	$\text{CaO}$	$\text{MgO}$	$\text{Na}_2\text{O}$	$\text{K}_2\text{O}$	$\text{PbO}$
F	55.05	13.61	24.42	6.92	2.82	3.02	–
FP5	55.05	13.61	24.42	6.92	2.82	3.02	5
FP10	55.05	13.61	24.42	6.92	2.82	3.02	10
FP15	55.05	13.61	24.42	6.92	2.82	3.02	15

$$\alpha = \frac{d_g - d_b}{d_g}$$

where  $d_b$  and  $d_r$  are the bulk and the real densities of the fired sample containing foaming agent, respectively, and  $d_g$  is the bulk density of the fired foaming agent-free specimen.

The resultant microstructures were evaluated by a scanning electron microscope (Vega Tescan) after polishing and etching the specimens in a 5 vol.% HF solution for 15 s.

The crystallinity of the fired specimens was identified by X-ray diffractometers (Siemens-D500, JEOL JDS-8030).

The thermal analysis of the samples was carried out by simultaneous thermal analyses (NETZSCH 409) in two different atmospheres of air and argon using a heating rate of 10 °C/min.

The dilatometric softening point of the glasses was determined by a dilatometer (NETZSCH 402). The heating rate was 10 °C/min in this experiment. The wettability of glass with respect to  $\text{SiC}$  particles was determined by measuring the angles of contacts ( $\theta$ ) at 1200 °C by the sessile drop method [28].

## 3. Results and discussion

### 3.1. Thermal and physical properties of the glass foam

Fig. 1 depicts the DTA traces of the glasses obtained in an air atmosphere. The onset crystallisation temperature ( $T_0$ ) and crystallisation peak temperature ( $T_c$ ) of the glasses obtained from each DTA run and the dilatometric softening points ( $T_s$ ) obtained via the dilatometry method are shown in Table 2. This figure indicates that the crystallisation peak temperature of the glass gradually increases with increasing  $\text{PbO}$  content whereas the peak intensity decreases with the addition of  $\text{PbO}$ . Thus, the affinity of glasses for crystallisation reduces with the addition of  $\text{PbO}$ .

According to the XRD results, diopside and gehlenite were precipitated at 1000 °C in all glasses (Fig. 2).

Figs. 3–5 depict the bulk density, total porosity and foaming factor ( $\alpha$ ) of the  $\text{SiC}$ -containing glasses after sintering at a temperature range of 850–1000 °C. According to Figs. 3 and 4, the specimen FS2 showed a high bulk density and a low

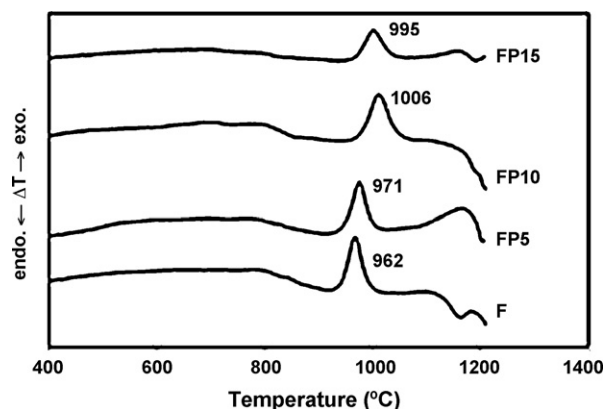


Fig. 1. DTA curves of glasses at a heating rate of 10 °C/min.

Table 2

Characteristic temperatures (°C) of glass F containing various amounts of PbO.

Glass	$T_s$	$T_0$	$T_c$	$T_0 - T_s$
F	815	913	962	98
FP5	–	926	971	–
FP10	725	951	1006	226
FP15	657	947	995	272

$T_s$ : dilatometric softening point;  $T_0$ , onset of crystallisation peak temperature;  $T_c$ , crystallisation peak temperature.

foaming factor ( $\alpha$ ), which are never appropriate characteristics for a foam material. However, by adding PbO, they were changed favourably. Accordingly, the bulk densities of specimens decreased with increasing temperature such that in FP10S2, it reached to its minimum values between 900 and 1000 °C. These trends are well matched with their total porosity-sintering temperature graphs (Fig. 5).

The development of foaming ability in the lead-bearing glasses was associated with a decrease of the crystallisation peak intensities of diopside, leading to a lower affinity for crystallisation (Figs. 1 and 2). These specifications of PbO-bearing glasses, which have been observed previously [29], permit the glass to react with silicon carbide particles and evolve enough gas required for foaming.

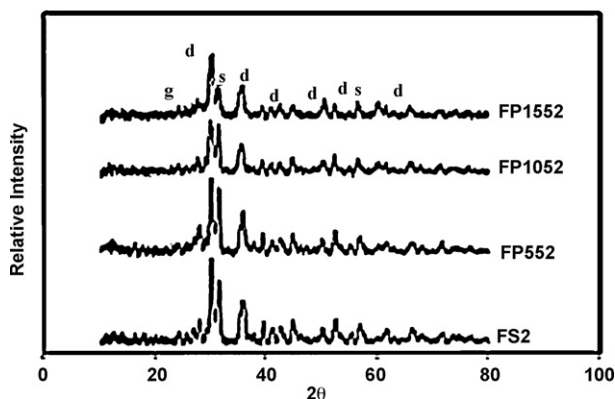


Fig. 2. XRD analysis illustrating the phases (d: diopside; g: gehlenite) present in fired glasses at 1000 °C.

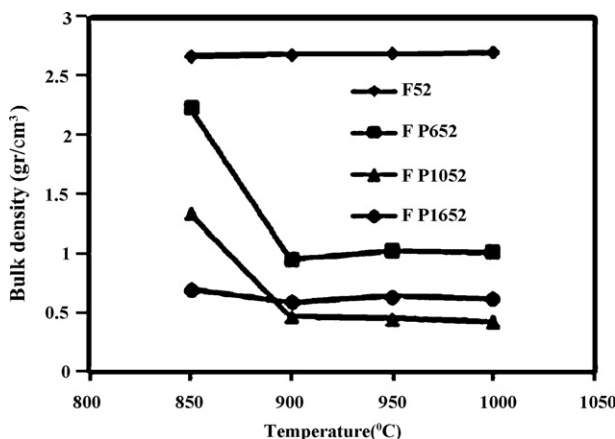


Fig. 3. Bulk density variations with heat treatment temperature.

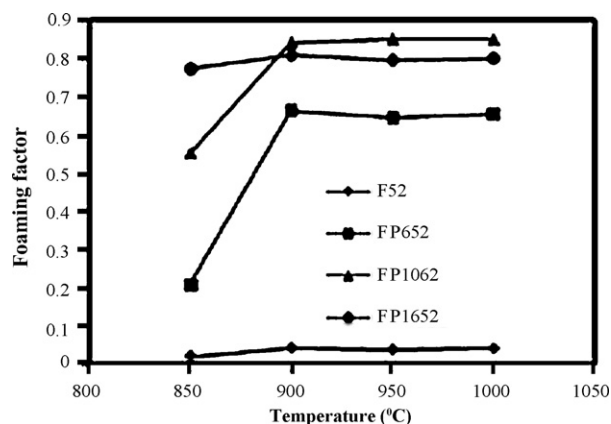


Fig. 4. Foaming factor variations with heat treatment temperature.

### 3.2. Foaming process

In a compacted glass–SiC body, the required oxygen for the foaming process can be supplied via two different sources: (a) the oxygen dissolved in the glass and (b) the atmosphere in which the sample is being fired [17]. To investigate the role of each mechanism, TG thermographs of the used SiC particles, SiC-free glass (FP15) and glass-containing SiC (FP15S2) were compared in oxidising (air) and neutral (argon) atmospheres (Fig. 6). The following equations show the oxidation of SiC at

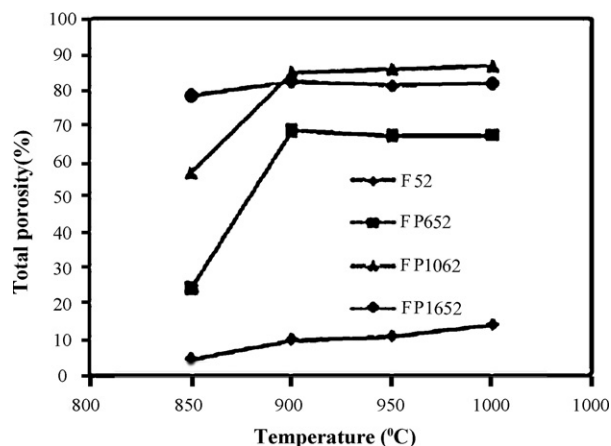


Fig. 5. Total porosity variations with heat treatment temperature.

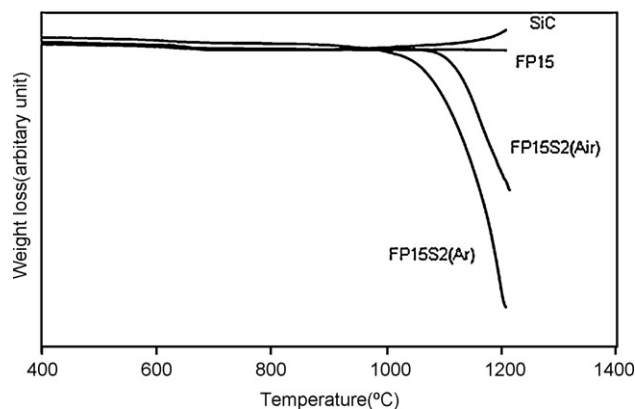


Fig. 6. TG thermographs of SiC, glass FP15 and specimen FP15S2 under air and argon atmospheres and a heating rate of 10 °C/min.

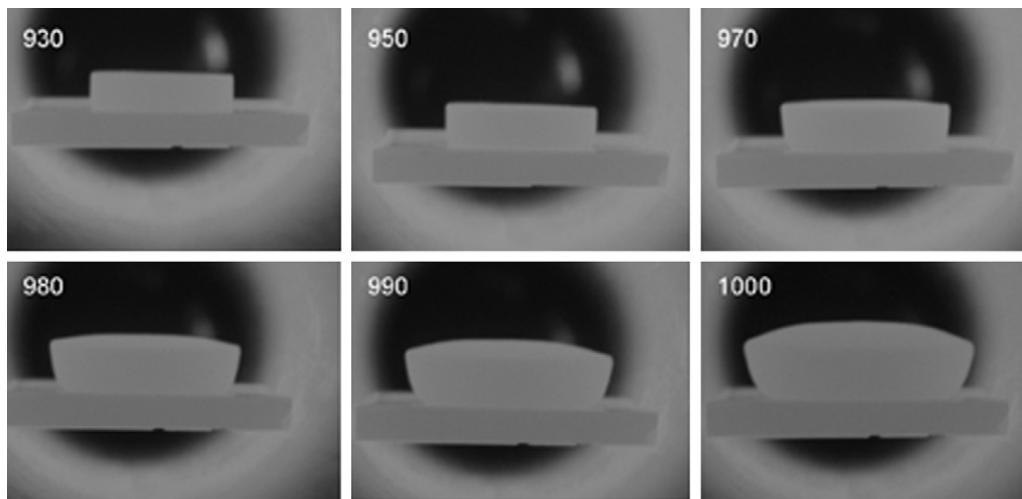


Fig. 7. Foaming behaviour of a compacted glass FP15S2 specimen during heating in an electric tube kiln with a heating rate of 10 °C/min.

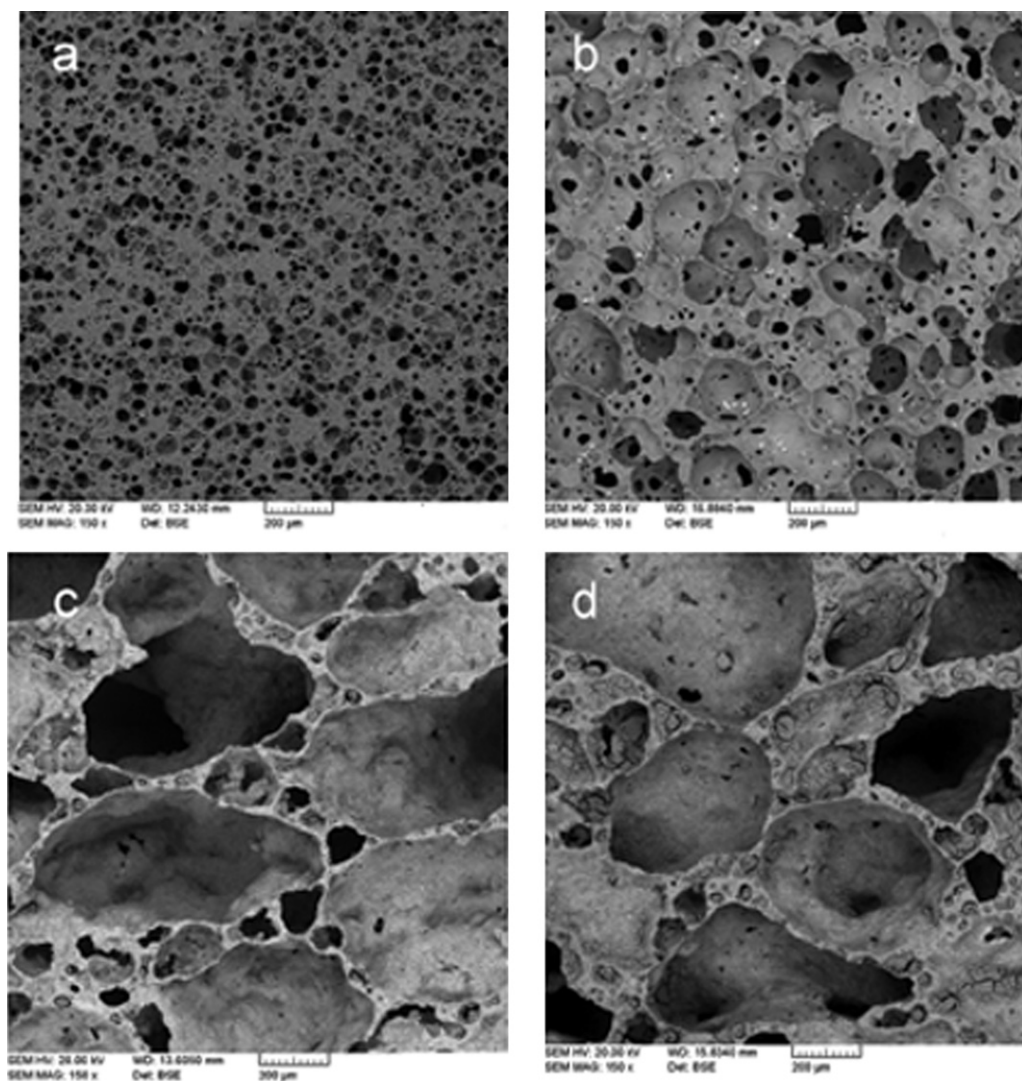
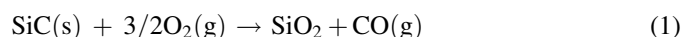


Fig. 8. An electron micrograph of FP10S2 glass–ceramic foam at (a)  $T = 850$  °C, (b)  $T = 900$  °C, (c)  $T = 950$  °C and (d)  $T = 1000$  °C.

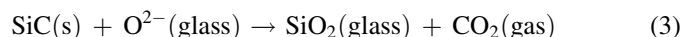


temperatures below (Eq. (1)) and above (Eq. (2)) 1400 °C, according to Village et al. [30]:



These reactions will be associated with weight gain and weight loss of the samples, respectively.

Fig. 6 indicates a negligible weight gain in the used SiC particles up to 1200 °C, when it was fired in air. In contrast, while the weight change of glass FP15 is negligible, the TG thermographs of FP15S2 show a high weight loss above 1000 °C in both oxidising and neutral atmospheres. This behaviour is probably due to the following reaction:



The higher temperature of initiation of weight loss in the sample fired in an air atmosphere was attributed to formation of a viscous silica glass film around each SiC particle, which delays reaction (3) relative to the other firing condition. This silica glass film was formed in the course of heating up the specimen in the TG apparatus.

Sample FP15S2 showed almost the same foaming behaviour from its own volume changes when it underwent firing at the same heating rate in an electric tube kiln in an oxidising atmosphere (Fig. 7). Accordingly, foaming was started at approximately 970 °C. However, regarding the related TG thermograph, the resulting gas phase might have been released from the specimen at higher temperatures, i.e., approximately 1000 °C, when the pressure was high enough to tear the walls of the closed pores.

The role of lead oxide in the foaming of the glasses was investigated more precisely by measuring the wettability and surface tension of the glasses. The results are presented in Table 3.

A lower surface tension and/or contact angle means a higher interfacial area of glass–SiC and hence a higher probability of reaction (3) occurring. The ultimate result is the formation of solid foam by bloating of the specimens. The present results certainly are accompanied by a fluxing effect of lead oxide in glasses, which plays a role in decreasing the glass viscosity, which is necessary for bloating phenomena to occur.

### 3.3. Microstructural evaluation

Fig. 8 shows SEM micrographs of the sample FP10S2 after firing in the 850–1000 °C interval. This figure shows that the cell size of the specimen increased with increasing firing temperature, probably because of the increasing gas pressure

Table 3

Wetting angle and surface tension of the glasses at 1200 °C.

Glass	Wetting angle (°)	Surface tension (dyn/cm)
F	85	402.75
FP10	60	377.3
FP15	55	366.16

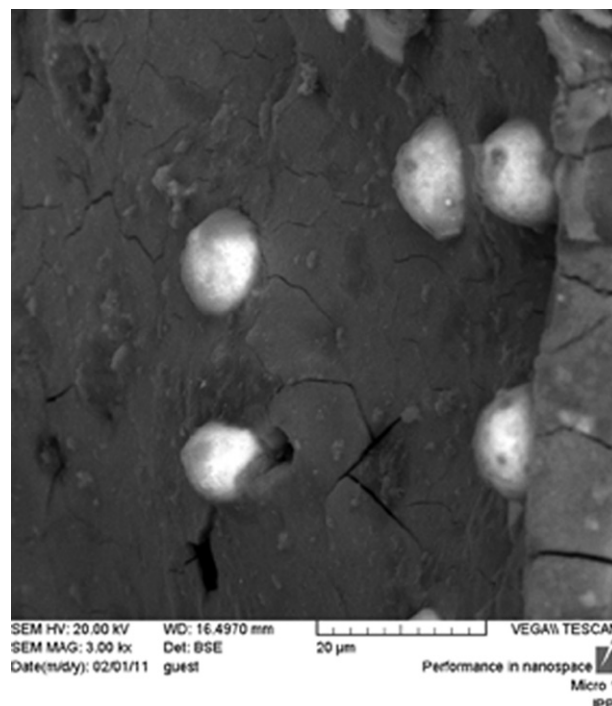
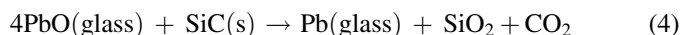


Fig. 9. Small droplets of lead oxide on the pore surface.

and decreasing glass viscosity with temperature, which brought about the pore coarsening, i.e., smaller pores likely dissolved in larger ones. This phenomenon is favoured by the decrease in the surface energy of the system [13]. Small white dots observed on the pore surfaces (Fig. 9) using EDS analysis (Fig. 10) consisted of Pb and O elements. Therefore, one can conclude that the dots were formed by the following reactions [7]:



The dots should precipitate in the vicinity of SiC–glass interfaces.

Fig. 11 shows the microstructures of the FP15S2 after sintering at 1000 °C. Accordingly, fine crystals of diopside and/or gehlenite became embedded in the glass matrix of the pore wall.

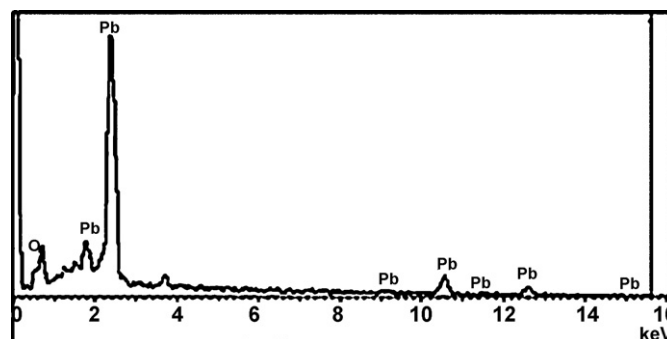


Fig. 10. An EDS spectrum of a droplet on the pore surface.

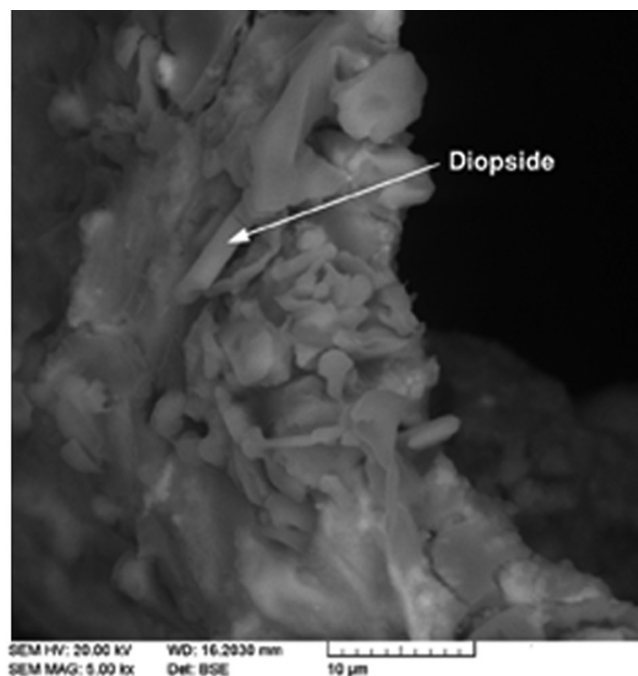


Fig. 11. A SEM micrograph of diopside crystals embedded in the glass matrix of a pore wall in FP15S2 glass–ceramic foam.

#### 4. Conclusions

- (1) PbO was required to improve the foaming behaviour of diopside-based glass–ceramic. The improvement in the foaming ability of the glass was associated with (a) the shift of the crystallisation peak temperatures to higher temperatures and (b) a decrease in the contact angle of the glass as a result of a decrease in the surface tension. These alterations in the glass were confirmed by a decrease in the DTA peak intensity.
- (2) Specific experiments demonstrated that bubbles were formed in the glass via the reaction between oxygen ions of the glass structure and the SiC particles and that this behaviour was independent of firing atmosphere. The reaction led to glass ceramic samples with bulk densities as low as  $0.5 \text{ g/cm}^3$ .

#### References

- [1] G. Scarini, G. Brusatin, E. Bernardo, Production technology of glass foams, in: M. Scheffler, P. Colombo (Eds.), *Cellular Ceramics. Structure, Manufacturing, Properties and Applications*, Wiley-VCH, Weinheim, Germany, 2005.
- [2] W.O. Lytle, Pittsburgh Plate Glass, USA, US Patent 2,215,223 (1940).
- [3] E. Bernardo, R. Cedro, M. Florean, S. Hreglich, Reutilization and stabilization of wastes by the production of glass foams, *Ceram. Int.* 33 (2007) 963–968.
- [4] E. Bernardo, G. Scarinci, Recycling of waste glasses into partially crystallized glass foams, *J. Porous. Mater.* 17 (2010) 359–365.
- [5] A.S. Llaudis, M.J.O. Tari, F.J.G. Ten, E. Bernardo, P. Colombo, Foaming of flat glass cullet using  $\text{Si}_3\text{N}_4$  and  $\text{MnO}_2$  powders, *Ceram. Int.* 35 (2009) 1953–1959.

- [6] D.U. Tulyaganov, H.R. Fernandes, S. Agathopoulos, J.M.F. Ferreira, Preparation and characterization of high compressive strength foams from sheet glass, *J. Porous. Mater.* 13 (2006) 133–139.
- [7] H.W. Gue, Y.X. Gong, S.Y. Gao, Preparation of high strength foam glass–ceramics from waste cathode ray tube, *Mater. Lett.* 64 (2010) 997–999.
- [8] E. Bernardo, Micro- and macro-cellular sintered glass–ceramics from wastes, *J. Eur. Ceram. Soc.* 27 (2007) 2415–2422.
- [9] E. Bernardo, G. Scarinci, S. Hreglich, Foam glass as a way of recycling glasses from cathode ray tubes, *Glass Sci. Technol.* 78 (2005) 7–11.
- [10] F. Mear, P. Yot, M. Cambon, R. Caplian, M. Ribes, Characterization of porous glasses prepared from cathode ray tube (CRT), *Powder Technol.* 162 (2006) 59–63.
- [11] F. Mear, P. Yot, M. Ribes, Effects of temperature, reaction time and reducing agent content on the synthesis of macroporous foam glasses from waste funnel glasses, *Mater. Lett.* 60 (2006) 929–934.
- [12] F. Mear, P. Yot, R. Viennois, M. Ribes, Mechanical behavior and thermal and electrical properties of foam glass, *Ceram. Int.* 33 (2007) 543–550.
- [13] E. Bernardo, F. Albertini, Glass foams from dismantled cathode ray tubes, *Ceram. Int.* 32 (2006) 603–608.
- [14] F. Mear, P. Yot, M. Cambon, M. Ribes, Elaboration and characterization of foam glass from cathode ray tubes, *Adv. Appl. Ceram.* 104 (2005) 123–130.
- [15] Z.-Y. Feng, X.-X. Xue, Y. Li, H. Yang, Preparation of foam glass–ceramic from oil shale residue, *Chin. J. Process Eng.* 8 (2008) 378–383.
- [16] H.R. Fernandes, D.U. Tulyaganov, J.M.F. Ferreira, Preparation and characterization of foams from sheet glass and fly ash using carbonates as foaming agents, *Ceram. Int.* 35 (2009) 229–235.
- [17] A.C. Steiner, Foam Glass Production from vitrified Municipal Waste Fly Ashes, Doctoral Thesis, Technische Universiteit Eindhoven, Dusseldorf, 2006.
- [18] H.R. Fernandes, D.U. Tulyaganov, J.M.F. Ferreira, Production and characterization of glass–ceramic foams from recycled raw materials, *Adv. Appl. Ceram.* 108 (2009) 9–13.
- [19] J.P. Wu, A.R. Boccaccini, P.D. Lee, M.J. Kershaw, R.D. Rawlings, Glass–ceramic foams from coal ash and waste glass: production and characterization, *Adv. Appl. Ceram.* 105 (2006) 32–39.
- [20] J.P. Wu, A.R. Boccaccini, P.D. Lee, R.D. Rawlings, Thermal and mechanical properties of a foamed glass–ceramic material produced from silicate wastes, *Glass Technol. Eur. J. Glass Sci. Technol. A* 48 (2007) 133–141.
- [21] B. Xu, K.M. Liang, J.W. Cao, Y.H. Li, Preparation of foam glass ceramics from phosphorus slag, *Adv. Mater. Res.* 105–106 (2010) 600–603.
- [22] Yu.A. Spiridonov, I.A. Orlova, Problems of foam glass production, *Glass Ceram.* 60 (2003) 313–314.
- [23] S.S. Akulich, B.K. Demidovich, V.I. Piletskii, Effectiveness of using nepheline concentrate in the manufacture of foam glass, *Glass Ceram.* 27 (1970) 86–88.
- [24] G.A. Khater, The use of Saudi slag for the production of glass–ceramic materials, *Ceram. Int.* 28 (2002) 59–67.
- [25] G.A. Khater, Glass–ceramics in the  $\text{CaO-MgO-Al}_2\text{O}_3\text{-SiO}_2$  system based on industrial waste materials, *J. Non. Cryst. Solids* 356 (2010) 3066–3070.
- [26] H. Xiao, Y. Cheng, Y. Yu, H. Liu, A study on the preparation CMAS glass–ceramics by in situ crystallization, *Mater. Sci. Eng. A* 431 (2006) 191–195.
- [27] M. Rezvani, B. Eftekhari-Yekta, M. Solati-Hashjin, V.K. Marghussian, Effect of  $\text{Cr}_2\text{O}_3$ ,  $\text{Fe}_2\text{O}_3$  and  $\text{TiO}_2$  nucleants on the crystallization behavior of  $\text{SiO}_2\text{-Al}_2\text{O}_3\text{-CaO-MgO(R}_2\text{O)}$  glass–ceramics, *Ceram. Int.* 31 (2005) 75–80.
- [28] P.C. Hiemenz, *Principle of Colloid and Surface Chemistry*, Marcel Dekker, New York, 1997, pp. 209–251.
- [29] B. Eftekhari-Yekta, V.K. Marghussian, Effect of  $\text{P}_2\text{O}_5$ ,  $\text{B}_2\text{O}_3$  and PbO on the sintering of quartz solid solution and gahnite glass–ceramics, *J. Eur. Ceram. Soc.* 36 (2001) 477–483.
- [30] M. Village, T. Sierra, F. Lucas, J.F. Fernandez, A.C. Caballero, Oxidation treatments for SiC particles and its compatibility with glass, *J. Eur. Ceram. Soc.* 27 (2007) 861–865.